Cardiovascular Drugs and Therapy (2021) 35:73–85
https://doi.org/10.1007/s10557-020-07064-z

ORIGINAL ARTICLE

Spermine Protects Cardiomyocytes from High Glucose-Induced Energy Disturbance by Targeting the CaSR-gp78-Ubiquitin Proteasome System

Yuehong Wang[1] · Yuwen Wang[2] · Fadong Li[1] · Xinying Zhang[1] · Hongzhu Li[1] · Guangdong Yang[3] · Changqing Xu[1] · Can Wei[1]

Accepted: 25 August 2020 / Published online: 12 September 2020
© Springer Science+Business Media, LLC, part of Springer Nature 2020

Abstract

Purpose To determine the mediation of spermine on energy metabolism disorder and diabetic cardiomyopathy (DCM) development as well as the underlying mechanisms.

Methods An in vitro model of DCM was established by incubating primary cultured neonatal rat cardiomyocytes with high glucose (HG). Spermine content was assessed by RP-HPLC. The protein levels were detected by western blot. Mitochondrial functions were analyzed using the respiratory chain complex assay kit and immunofluorescence staining.

Results The endogenous content of spermine was decreased in the HG group, and the protein levels of ornithine decarboxylase, respiratory chain complex (I–V), mitochondrial fusion-related protein (Mfn1, Mfn2), Cx43, N-cadherin, CaSR, and β-catenin (in cytomembrane) were also down-regulated by HG. In contrast, the protein levels of spermine-N1-acetyltransferase, gp78, Fis1, Drp1, and β-catenin were up-regulated by HG. Meanwhile, we observed that HG increased ubiquitination levels of Mfn1, Mfn2, and Cx43, decreased membrane potential (ΔΨm), and the opening of mitochondrial permeability transport pore (mPTP) followed by intracellular ATP leakage. The supplement of spermine or siRNA-mediated knockdown of gp78 significantly alleviated the detrimental effects of HG, while downregulation of CaSR aggravated the development of DCM. We further confirmed that the lower level of spermine by HG activates the gp78-ubiquitin-proteasome pathway via downregulation of CaSR protein level, which in turn damages mitochondrial gap junction intercellular communication and leads to reduced ATP level.

Conclusion The protective role of spermine on energy metabolism disorder is based on higher CaSR protein level and lower gp78 activation, pointing to the possibility that spermine can be a target for the prevention and treatment of DCM.

Keywords Spermine · Diabetic cardiomyopathy · Gp78 · ATP · Connexin43

Abbreviations

AMFR	autocrine motility factor receptor
ATP	adenosine triphosphate
ATP5F1	ATP synthase F(0) complex subunit B1
COX5A	cytochrome c oxidase subunit Va
Cx43	connexin-43
DCM	diabetic cardiomyopathy
Drp1	dynamin-related protein 1
ERAD	endoplasmic reticulum related degradation
Fis1	fission 1
GJIC	gap junction intercellular communication
GSK-3β	glycogen synthase kinase 3 beta
HG	high glucose
Hsp70	heat-shock protein 70
Mfn	mitofusin
ND1	NADH dehydrogenase subunit 1
ODC	ornithine decarboxylase
p-β-catenin	phospho-β-catenin
p-Cx43	phospho-connexin-43
p-GSK-3β	phospho-glycogen synthase kinase 3 beta

Yuehong Wang and Yuwen Wang contributed equally to this work.

✉ Can Wei
canwei528@163.com

[1] Department of Pathophysiology, Harbin Medical University, Baojian Road, Harbin 150081, China

[2] Department of Clinical Laboratory, The Second Affiliated Hospital of Harbin Medical University, Harbin 150000, China

[3] Departemnt of Chemistry and Biochemistry, Laurentian University, Sudbury P3E 2C6, Canada

SDHA	succinate dehydrogenase complex flavoprotein subunit A
SLDT	scrape-loading dye transfer technique
SSAT	spermine-N1-acetyltransferase
TBST	tris-buffered saline-Tween 20
UQCRQ	ubiquinol-cytochrome c reductase
VDAC	voltage-dependent anion channel

Introduction

Diabetic cardiomyopathy (DCM) refers to a myocardial disease in diabetic patients that is not often related with coronary heart disease, hypertensive heart disease, and other heart diseases [1, 2]. DCM is characterized by oxidative stress, calcium metabolism disorder, mitochondrial dysfunction, inflammation, and fibrosis on the basis of persistent metabolic disorders and microangiopathy. Uncontrolled DCM will lead to extensive focal myocardial necrosis, heart failure, shock, and even sudden death [3–5]. It has been reported that more than 2/3 of diabetes patients pass away due to heart failure caused by DCM [6]. Despite the high incidence of DCM, the exact mechanism of DCM remains unclarified, and effective prevention and treatment methods are lacking.

One of the main features of DCM is myocardial diastolic and systolic dysfunction, which are associated with energy metabolism disorders and calcium homeostasis imbalance [7, 8]. Mitochondria are the energy "power plant" of cells and produce a large amount of ATP via the mitochondrial respiratory chain. The normal structure of mitochondria depends on the interaction and dynamic balance of mitochondrial fusion protein (Mfn1, Mfn2), mitochondrial fission protein (Fis1), and dynamin-related protein 1 (Drp1) [9]. Blocking of mitochondrial fusion can lead to decreased mitochondrial oxygen consumption and membrane potential, while disrupted mitochondrial fission can affect mitochondrial recruitment and location [10]. Taken together, this evidence suggest that the structural damage of mitochondria is tightly related with disrupted ATP synthesis.

Connexin proteins are the structural basis for transferring small molecule nutrients, energy, and electrical signals between myocardial cells [11, 12]. Among them, connexin 43 (Cx43) is the most important connexin protein that constitutes the gap junction intercellular communication (GJIC) between cardiomyocytes [13]. The binding of Cx43 with N-cadherin and beta-catenin is necessary for the formation of complete GJIC [14, 15]. Recent studies have shown that the destruction of GJIC would lead to ATP leakage [8, 16].

We previously found that the damage of cardiomyocytes in diabetic rats and high glucose (HG)-treated primary cultured neonatal cardiomyocytes are associated with decreased CaSR protein level, calcium homeostasis imbalance, oxidative stress, endoplasmic reticulum stress, and increased apoptosis [17, 18]. Spermine, an agonist of CaSR, plays a protective role in myocardial functions. However, the involvement of spermine in the development of DCM and its protective role in mitochondrial functions and energy metabolism of DCM remain unexplored.

In this experiment, we established an in vitro model of DCM by incubating primary cultured neonatal rat cardiomyocytes with HG for 48 h. We observed the changes of endogenous spermine content upon HG treatment and further demonstrated the protective roles of exogenous spermine on energy metabolism disorder in DCM, pointing to the possibility that spermine can be a target for preventing and treating DCM.

Materials and Methods

Isolation and Culture of Neonatal Rat Cardiomyocytes

The isolation and primary cultures of cardiomyocytes from neonatal Wistar rats (1–3 d) were prepared as previously described [19]. Briefly, the hearts were cut into pieces on the super-clean workbench, digested with trypsin (Beyotime Biotechnology, Shanghai, China) for 8 min, then the Dulbecco's modified Eagle's medium (DMEM) (Gibco, Grand Island, NY) with 10% fetal bovine serum (FBS), 100 U/ml penicillin, 100 mg/ml streptomycin, and 5.5 mM glucose was added to terminate the digestion. After repeating the process eight times, the cells were collected by centrifugation at 600 *g* at 4 °C for 10 min. The cells were then cultured in a humidified atmosphere with 5% CO_2 at 37 °C for 2 h, the attached cells were discarded and the unattached cardiomyocyte cells were continuously cultured in a collagen-coated petri dish with DMEM (5.5 mM glucose, 10% FBS). The primary cardiomyocytes were successfully separated as evidenced by the morphology of spindle-shaped, triangular, and irregular star-shaped. All the experiments were approved by the Animal Care Committee for the Use of Experimental Animals at Harbin Medical University (Heilongjiang, China).

Experimental Protocols

The cultured cells were randomly divided into four groups: (1) Control group (Control): cardiomyocytes cultured with DMEM (5.5 mM glucose, 10% FBS); (2) High glucose group (HG): cardiomyocytes cultured with DMEM containing HG (40.0 mM glucose); (3) HG + spermine group (HG + Sp): 5 μM spermine (Sigma, St. Louis, MO, USA) was added to the medium for 30 min before HG incubation. (4) HG + NPS R568 group (HG + NPS R568): 5 μM NPS R568 (Sigma), as a specific agonist of CaSR, was added to the medium for 30 min before HG incubation. Then all the cardiomyocytes were incubated for 48 h.

Myocardial Spermine Content Detection by RP-HPLC

Spermine was obtained from Sigma. Myocardial spermine content was determined by reversed-phase high performance liquid chromatography (RP-HPLC) using ODS-C18 columns, as previously described [19]. Spermine was used as positive controls, and benzoyl chloride was used as a derivative reagent. Derivatization was conducted at 50 °C for 8 h, mobile phase as methanol/water (45/55), flow rate as 1.0 mL/min, and detection wavelength at 234 nm. The spermine content was determined by the size of the peak area.

Plasma Membrane Protein Fractionation

The cells were scraped from the plates into ice-cold PBS containing protease and phosphatase inhibitors. Plasma membrane-enriched fractions were isolated by filtration and differential density centrifugation with a commercial kit (Invent Biotechnologies, Plymouth, MN, USA). The procedure isolated post-nuclear total membrane proteins that were further separated into enriched plasma membrane and organelle fractions. The purity of each fraction was determined by western blotting with specific antibodies.

Mitochondria Isolation

The mitochondria were isolated following a previous method with slight modifications [8, 20]. Briefly, all the cells were isolated by centrifugation and washed three times with PBS at 4 °C. Cells were resuspended with ice-cold hypotonic buffer (10 mM Tris-HCl, pH 7.6) containing protease and phosphatase inhibitor cocktails. The cell homogenate was then gently passed 30 times through a 26 G 1/2 needle using a 1 mL syringe and centrifuged at 800 *g* for 10 min at 4 °C. The supernatant was collected in a 1.5 mL microcentrifuge tube and centrifuged again at 800 *g* for 10 min at 4 °C. The supernatant containing the crude mitochondria was transferred to a new tube with 1.5 M sucrose solution (the final sucrose concentration was 180 mM), and the mixtures were then centrifuged at 14,000 *g* for 10 min to get the precipitation of mitochondria. Finally, the specific lysis solution for mitochondria (Beyotime Biotechnology, ShangHai, China) was used to extract the mitochondria related proteins.

Scrape-Loading Dye Transfer

The scrape-loading dye transfer technique (SLDT) was used to detect GJIC functions [21]. In short, cardiomyocytes (1×10^5 cells/dish) were grown in a 35 mm petri dish and rinsed three times with PBS containing 0.01% Ca^{2+} and 0.01% Mg^{2+}. Then, 15 mL PBS containing 0.05% Lucifer yellow CH (Molecular Probes, Thermo Fisher Scientific Inc., USA) were added to cover the dish bottom and several scratches were made on the bottom of the dish using a scalpel. The cells were incubated in the dye solution for 5 min and then rinsed with PBS containing Ca^{2+} and Mg^{2+}. Finally, the cells were fixed with 4% paraformaldehyde and observed using a fluorescence microscope (Olympus IX81, Olympus Corporation). Experiments were repeated three times independently.

Mitochondrial Respiratory Chain Complex Activity Assay

Mitochondria were extracted from neonatal cultured rat primary cardiomyocytes samples, as previously described [8, 20, 22, 23]. The activities of respiratory chain enzyme complexes I, II, III, IV, and V (C–I, C–II, C–III, C–IV, C–V) in mitochondria were assayed using the respiratory chain complex assay kit (GENMED, San Diego, CA, USA) and UV–VIS spectrophotometer (SHIMADZU, Japan). For C–I, the reaction time was 3 min, for C–IV, the reaction time was 1 min, and for C–II, C–III, and C–V, the reaction times were 5 min. All assays were performed at least three times. The protein concentration of each sample was detected by a BCA assay (Beyotime Biotechnology, Shanghai, China). The activity of each complex was normalized to the total protein concentration.

Determination of Mitochondrial Membrane Potential (Δψm)

Δψm was detected with a mitochondrial membrane potential assay kit (Santa Cruz, Bergheimer, Germany). The cells were incubated in JC-1 dye at 37 °C for 30 min in the dark and then washed three times with PBS. The fluorescence intensity was measured with a fluorescent microscope (Olympus IX81) at the excitation wavelength of 488 nm. JC-1 monomer emits the green fluorescence at 530 nm emission wavelengths and JC-1 aggregate emits the red fluorescence at 590 nm emission wavelengths. The ratio of red/green JC-1 was then calculated by using Image J software. After the fluorescent image was converted into an 8-bit black-and-white image, the optical density value was taken as fluorescence intensity. The decline or rise of the ratio represents the decrease or increase in Δψm. All experiments were repeated three times independently.

Assay of Mitochondrial Permeability Transition Pore (mPTP) Opening

Co-incubating Calcein-AM (Santa Cruz, Bergheimer, Germany) and cobalt chloride (Sigma Chemical Co., St. Louis, MO, USA) was utilized to detect the changes of mPTP opening. Cardiomyocytes were seeded in a 35 mm petri dish (2×10^5 cells/dish). After different treatments, the cells were stained with 2 μM Calcein-AM in the presence of 5 mM cobalt chloride for 30 min at 37 °C in the dark. The

fluorescence intensity was tested by using a fluorescence microscope (Olympus IX81) at 488 nm excitation and 525 nm emission wavelengths. The fluorescence intensity was calculated with Image J software. After the fluorescent image was converted into an 8-bit black-and-white image, the optical density value was taken as fluorescence intensity. Experiments were repeated at least three times independently.

MitoTracker Staining

Cardiomyocytes (1×10^5 cells/dish) were cultured in a 35 mm petri dish. After treatments, the cells were stained with 300 nM MitoTracker Deep Red FM (Molecular Probes, Thermo Fisher Scientific Inc., USA) for 20 min in the dark. Mitochondria were imaged by using a fluorescence microscope (Olympus IX81) and the average length of mitochondria was calculated using Image J (National Institutes of Health, USA). According to the official guidelines, the MiNA plug-in in ImageJ was used to analyze the mitochondrial length. The average mitochondrial length in the control group was set as 100%. Experiments were repeated three times independently.

Measurement of ATP Concentration

The concentration of ATP in cell lysate was measured by ATP Assay Kit (Beyotime Biotechnology, ShangHai, China) and Luminoskan™ Ascent (Thermo Fisher Scientific Inc., USA). Briefly, the primary neonatal cultured rat cardiomyocytes (1×10^5 cells/dish) were cultured in a 35 mm petri dish. After 48 h treatment, the cells were collected and then lysed with lysis buffer in the kit. The amount of ATP concentration for each sample was determined with an ATP calibration curve and expressed in pmol/μg protein.

To evaluate the concentration of extracellular ATP, the culture medium was measured by a previous method with slight modifications [8, 24]. Briefly, the primary neonatal cultured rat cardiomyocytes (1×10^5 cells/dish) were seeded in a 35 mm petri dish. Prior to measurement of the extracellular ATP levels, culture medium was removed, cardiomyocytes were washed twice with Hank's balanced salt solution and incubated for 5 min at 37 °C, in 0.2 mL of Hank's. After 48 h of different treatments, the medium was collected and ATP release was measured by the luciferin–luciferase assay with an ATP Assay Kit, following the manufacturer's instructions (Beyotime Biotechnology). A calibration curve was constructed using ATP standards and used to calculate ATP levels in test samples and expressed in pmol/μg protein.

Immunoblotting

Total protein from cardiomyocytes was extracted using Minute™ Total Protein Extraction Kit (Invent Biotechnologies, Plymouth, MN, USA) and proteins concentration was quantified using BCA Protein Assay Kit (Solarbio, Beijing, China). After quantification and denaturation, equal amounts of protein samples were electrophoresed in SDS-polyacrylamide gel and transferred onto PVDF membranes (Millipore, Schwalbach, Germany). The following primary antibodies were used in this experiment: ODC, SSAT, CaSR, Mfn1, Mfn2, Cx43, P-Cx43, cleaved-caspase 3 (Santa Cruz Biotechnology, Dallas, TX, USA); Drp1, β-catenin, p-β-catenin, N-cadherin, GSK-3β, p-GSK-3β antibodies (Cell Signaling Technology, Danvers, MA, USA); gp78, Hsp70, UQCRQ1, ND1, ATP5, COX5A, SDHA, β-actin (Proteintech, Wuhan, China). The CaSR, ODC, and SSAT antibodies were diluted as 1:250, the other primary antibodies were diluted as 1:1000 and incubated with the membrane overnight at 4 °C. Subsequently, a 1:10000 dilution of the secondary antibody (ZSGB-BIO, Beijing, China) was added to the membrane. The signals were detected using the Enhanced Chemiluminescent (ECL) kit (HaiGene, Harbin, China) and the Multiplex Fluorescent Imaging System (ProteinSimple, California, USA). The intensities of protein bands were quantified by a Bio-Rad ChemiDocTM EQ densitometer and Bio-Rad Quantity One software (Bio-Rad Laboratories, Hercules, CA, USA). VDAC was used to confirm equal mitochondria loading. Na^+, K^+ ATPase was used as an equal cellular membrane control and histone H3 as an equal nucleus loading. β-actin was employed to confirm equal cytosol loading.

Immunoprecipitation

After various treatments, the cells were collected and lysed. The lysates were collected by centrifugation at 14000 *g* for 20 min and then immunoprecipitated with 2 μg specific antibody against β-catenin or N-cadherin (Cell Signaling Technology) overnight at 4 °C. Afterward, the mixtures were coupled to Protein A/G Magnetic Beads (Selleckchem, Houston, TX, USA) for 2 h.

siRNA Transfection

Cardiomyocytes were seeded in a 35 mm petri dish and maintained in the absence of antibiotic culture medium for 24 h before transfection. The cells were transfected with control siRNA (Con-siRNA), gp78-siRNA, and CaSR-siRNA (Santa, Dallas, TX, USA) using Lipofectamine™ 3000 transfection reagent from Invitrogen™ (Thermo Fisher Scientific Inc., Scotland, UK). siRNA and the transfection reagent complex were added to the reduced serum media (Gibco™ Opti-MEM™, Thermo Fisher Scientific Inc., UK) for 8 h, the transfection was continued in normal medium containing 10% serum.

Ubiquitylation Assay In Vitro

A proteasome inhibitor MG132 (Selleckchem, Houston, TX, USA) was added to the cells for 6 h prior to collection. The cell lysates were processed with pull-down assays using an anti-ubiquitin antibody followed by immunoblotting with anti-Mfn1, anti-Mfn2 or anti-Cx43.

Statistical Analysis

Statistical analyses were performed using SPSS 21.0 software. All data were presented as means ± standard errors of the means (SEM). One-way analysis of variance (ANOVA) followed by the Student–Newman–Keuls test was used for statistical analyses of three or more groups. Student's *t* test was applied to analyze statistically significant differences between two groups. A $p < 0.05$ was considered statistically significant. GraphPad Prism was used for mapping and curve fitting.

Results

HG Lowers Endogenous Spermine Content and Apoptosis in Primary Neonatal Rat Cardiomyocytes

We first measured the content of endogenous spermine and the protein levels of ornithine decarboxylase (ODC, the key enzymes of polyamine synthesis) and spermine-N1-acetyltransferase (SSAT, the key enzymes of polyamine catabolism) in the primary cardiomyocyte exposed to 40 mM HG. The results showed that endogenous spermine content and ODC protein level were decreased but SSAT protein level was increased in the HG group (Fig. 1a and b). We then found that gp78 and cleaved-caspase3 protein levels were stimulated by HG, which were significantly reversed by exogenous spermine co-incubation (Fig. 1c).

Exogenous Spermine Prevents HG-Caused Mitochondrial Dysfunctions

To reveal the effects of the low level of endogenous spermine on mitochondrial structure and function damaged by HG, we

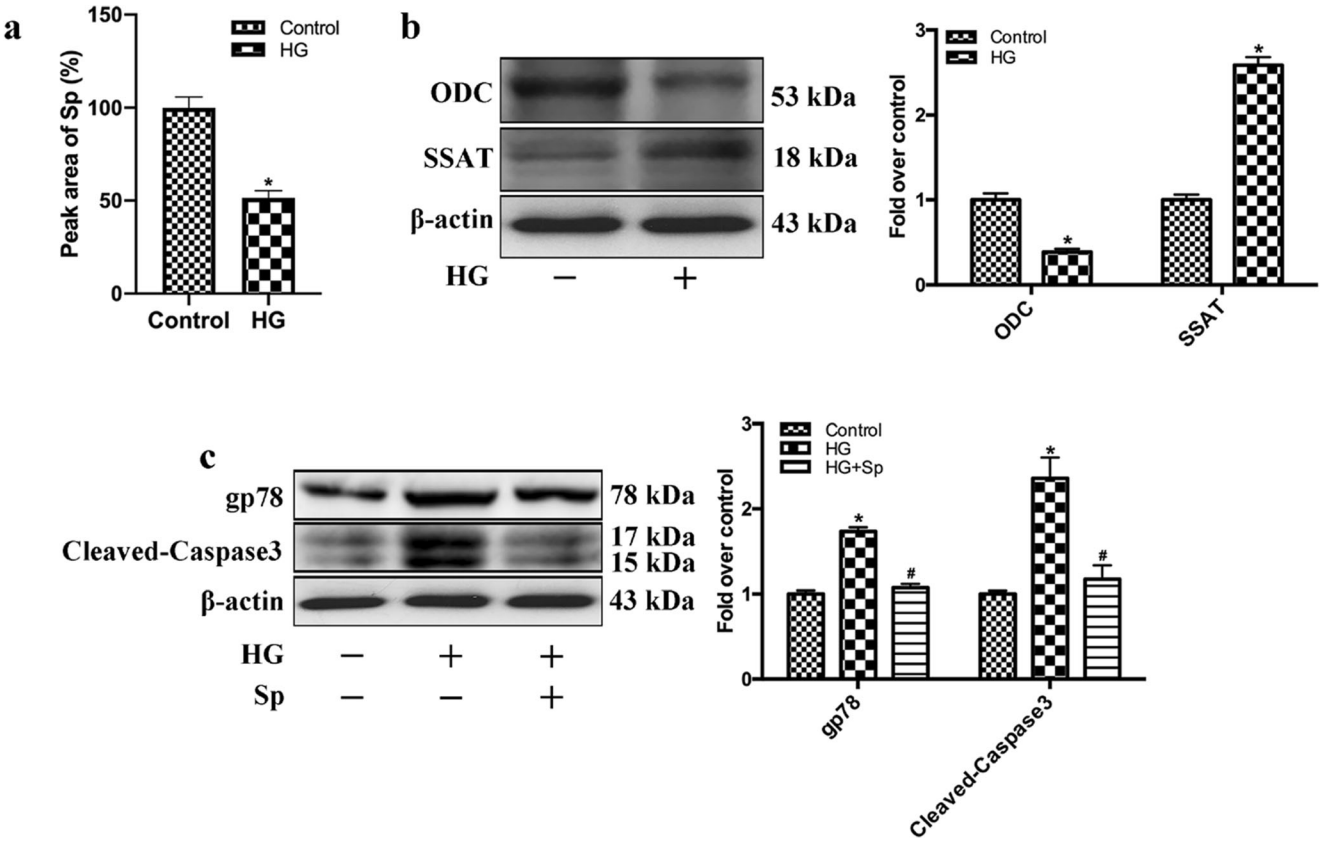

Fig. 1 The effect of HG on spermine content and apoptosis in primary neonatal cultured rat cardiomyocytes. The cardiomyocytes cultured in the control group (5.5 mM) and HG group (40.0 mM) with or without 5 μM spermine for 48 h were collected for analysis of polyamine metabolism and apoptosis. **a** Representative peak spectrogram of spermine content in cardiomyocytes by RP-HPLC; **b** Representative western blot of ODC and SSAT protein levels in cardiomyocytes and the protein levels normalized by β-actin; **c** Representative western blot of gp78 and cleaved caspase-3 levels in cardiomyocytes and the protein levels normalized by β-actin. All data expressed as means ± SE ($n = 3$). $^{*}p < 0.05$ vs. Control group; $^{\#}p < 0.05$ vs. HG group

analyzed the changes of mitochondrial structure-associated proteins and intracellular ATP contents. The levels of mitochondrial fusion-related proteins (Mfn1 and Mfn2) were decreased, while fission-related proteins (Fis1 and Drp1) levels were increased in the HG group (Fig. 2a). Mitochondrial morphology was further determined by staining the cells with Mito-Tracker, a mitochondria-specific probe [25]. The red fluorescence was widely and strongly distributed in the control group, but was fragmented in the HG group (Fig. 2b). Exogenous spermine treatment could prevent HG-altered levels of mitochondrial fission and fusion-related proteins (Fig. 2a and b). In comparison with the control (100%), the mitochondrial length in the HG group was decreased to 22.42 ± 2.57%, while it was increased to 85.43 ± 7.67% by spermine pretreatment (Fig. 2b). Mitochondrial damage could lead to the opening of mPTP, which would further result in the loss of ΔΨm [26]. Calcein-AM cobalt technology was used to detect the level of mPTP opening [8]. The fluorescence intensity of the control group was set as 100%, which was lowered to 34.61 ± 1.45% in HG group but increased to 65.39 ± 3.14% under exogenous spermine pretreatment (Fig. 2c). JC-1 exists as the polymers and presents red fluorescence under normal ΔΨm, which can be converted to monomers and emits green fluorescence when ΔΨm is declining. The red/green fluorescence ratio in the control group was set as 100%, the ratio was significantly decreased to 41.19 ± 5.22% in the HG group, and reversed to 82.48 ± 6.18% after spermine co-incubation (Fig. 2d). These results suggest that spermine protects HG-caused structural and functional disruption of mitochondria in cardiomyocytes.

We next found that HG significantly decreased the intracellular ATP concentration, while exogenous spermine could abolish this change (Fig. 3a). Heat shock protein 70 (Hsp70) is generally regarded as a marker of stress response. We found that Hsp70 protein level was significantly up-regulated in the HG group (Fig. 3b). The proton-transferring ability of mitochondrial respiratory chain is crucial for ATP generation [27]. We then measured the protein levels and activities of mitochondrial respiratory chain complexes (I–V) related proteins (ND1, SDHA, UQCRQ1, COX5A, and ATP5). Compared with the control group, each complex's protein level and activity was decreased in the HG group but reversed by the treatment with exogenous spermine (Fig. 3b and c). The results indicate that spermine protects mitochondrial functions by inhibiting stress response and stabilizing the mitochondrial respiratory chain.

Exogenous Spermine Alleviates HG-Induced Damage of Gap Junction Intercellular Communication (GJIC)

The cell membrane-associated gap junction proteins were further analyzed. We found that HG inhibited the protein levels

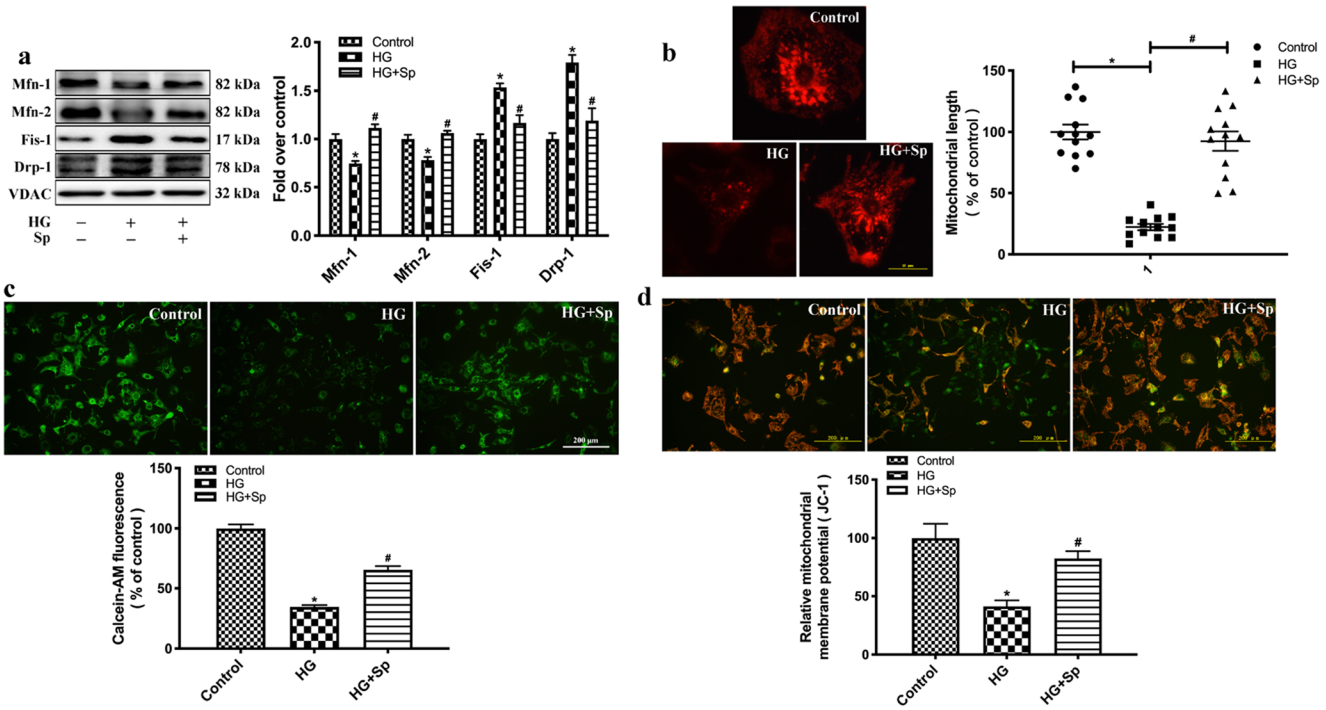

Fig. 2 Effects of HG and spermine on the mitochondrial structure. **a** Representative western blot of Mfn1, Mfn2, Fis1, and Drp-1 compared with VDAC protein level in cardiomyocytes. The cells were exposed to HG in the presence of 5 μM spermine for 48 h. **b** Morphology of mitochondria was detected using Mito-Tracker and photos were taken using fluorescence microscopy. Scale bars = 10 μm ($n = 12$). **c** The average length of mitochondria in each group were calculated (n = 12). **d** Calcein–AM was used to stain the cells to measure the changes of mPTP opening. The images were obtained by fluorescent microscopy ($n = 10$). **e** Δψm was measured using JC-1 staining and photos were taken using fluorescence microscopy. Scale bars = 200 μm. The average fluorescence intensities were expressed as the ratio of red to green (n = 10). *$p < 0.05$ vs. Control group; #$p < 0.05$ vs. HG group

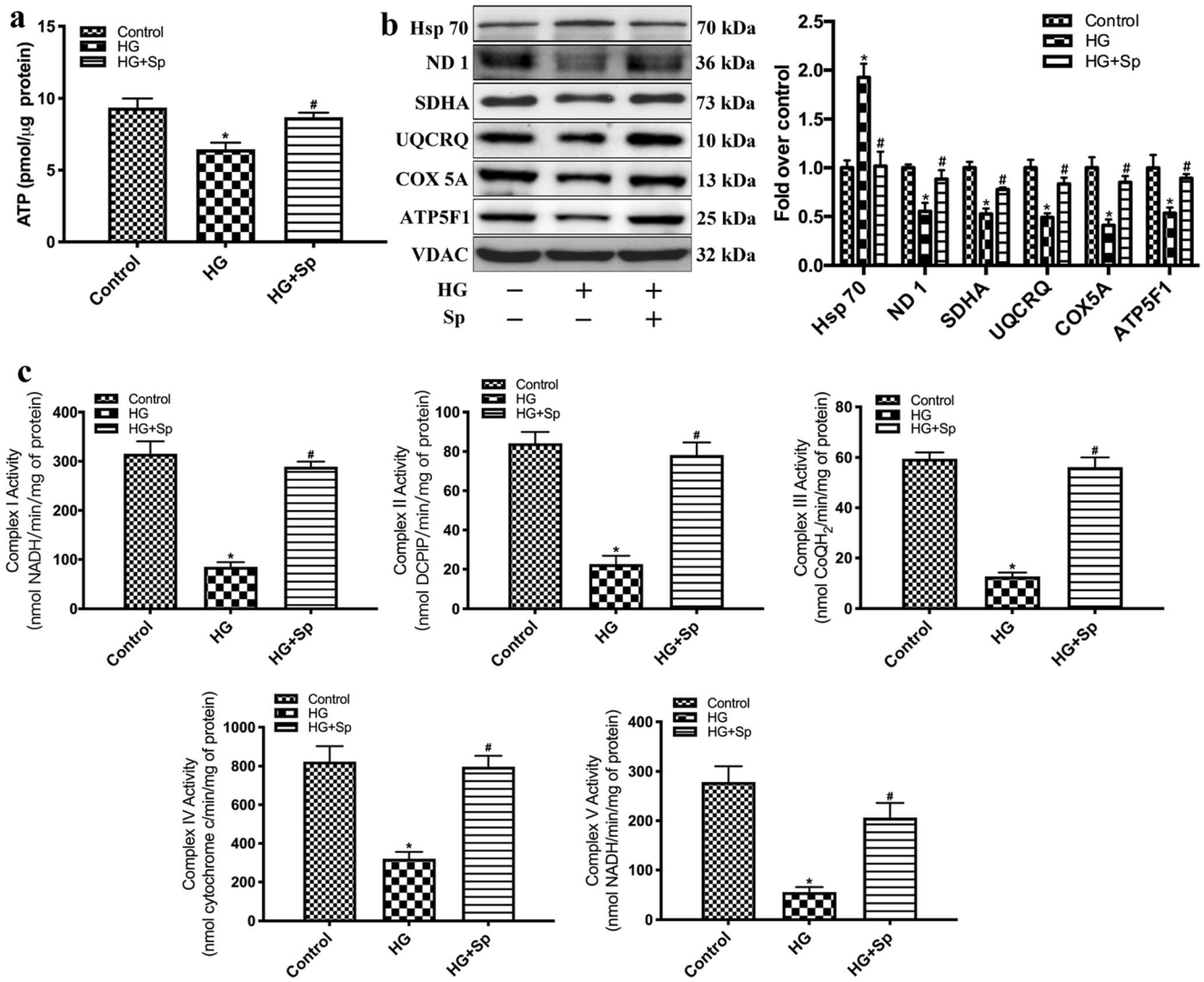

Fig. 3 Spermine attenuates HG-induced mitochondrial dysfunction. The cardiomyocytes were cultured in the control group (5.5 mM) and HG group (40.0 mM) with or without 5 μM spermine for 48 h. **a** The concentration of intracellular ATP was detected by chemiluminescence ($n = 3$). **b** Representative western blot of Hsp70, ND1, SDHA, UQCRQ, COX5A, and ATP5F1 in comparison with VDAC protein level in cardiomyocytes ($n = 3$). **c** Activities of complex (I–V) were detected by UV Spectrophotometry ($n = 4$). $^{*}p < 0.05$ vs. Control group; $^{\#}p < 0.05$ vs. HG group

of β-catenin, N-cadherin, and Cx43 but induced the phosphorylation of Cx43 (Fig. 4a). Scrape-loading dye transfer technique (SLDT) showed that the green fluorescence was widely distributed in the control group but only concentrated at the scratch marks in the HG group (Fig. 4b). Meanwhile, the extracellular ATP content was significantly increased in the HG group (Fig. 4c). We further tested the changes of the GJIC-related signaling pathway. The protein levels of β-catenin in cytoplasm (Cyto-β-catenin) and nucleus (N-β-catenin) and GSK-3β phosphorylation were significantly increased in the HG group; however, the phosphorylation of β-catenin was decreased by HG (Fig. 5). These detrimental effects of HG on GJIC could be reversed by the supplement of exogenous spermine, pointing to a critical role of spermine in maintaining the structure and function of GJIC.

Exogenous Spermine Alleviates HG-Induced Cardiomyocyte Damage Via Inhibiting gp78 Activation and up-Regulating CaSR Protein Level

To explore the involvement of gp78 in spermine-protected cardiomyocyte damage, siRNA was used to knock-down gp78 (Fig. 6a). Compared with the control group, the addition of spermine or gp78 knockdown significantly abolished HG-induced ubiquitylation of Mfn1, Mfn2, and Cx43 (Fig. 6b). These data suggest that the gp78-ubiquitin proteasome system may mediate the protective role of spermine on HG-induced DCM. It was previously reported that CaSR improves myocardial energy metabolism by inhibiting the gp78 protein level [8]. We also found here that HG decreased the CaSR protein level but significantly induced the gp78 level, while these changes

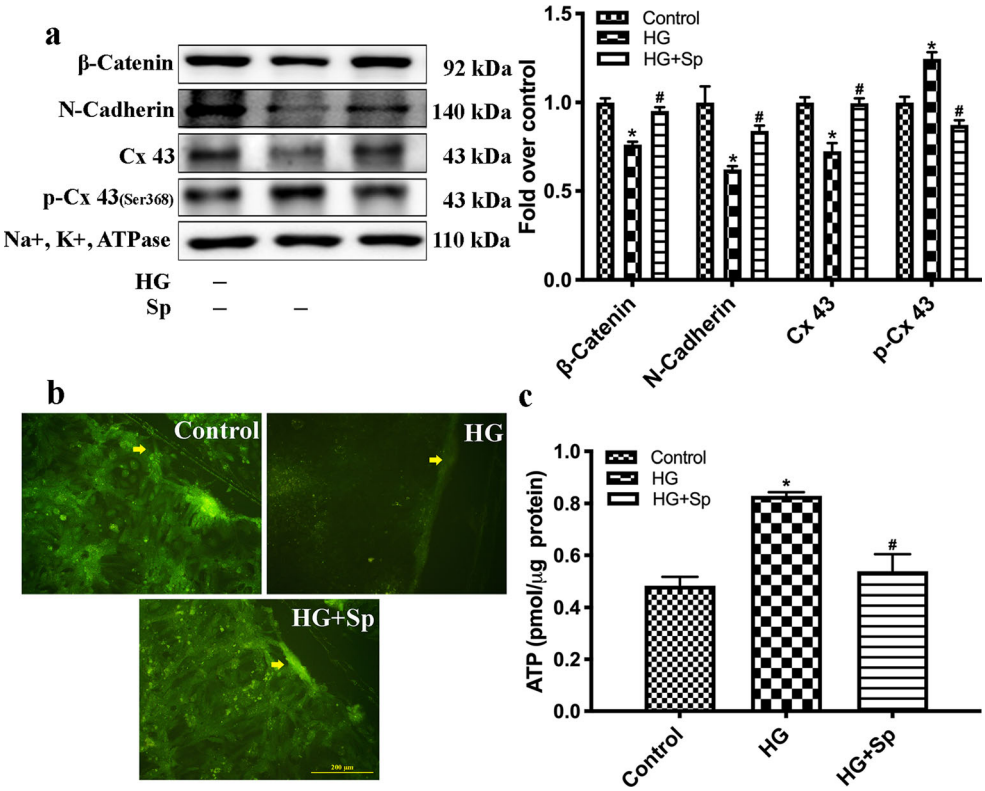

Fig. 4 Exogenous spermine stabilizes the function of the cell gap junction. **a** Representative western blot of β-catenin, N-cadherin, and Cx43 compared with Na^+, K^+-ATPase protein level in cardiomyocytes cytomembrane exposed to HG in the presence of 5 μM spermine (n = 3). **b** The function of GJIC was measured using the scrape-loading dye transfer technique (SLDT) and photoed using fluorescence microscopy. Scale bars = 10 μm (n = 3). The yellow arrow represents the scratch. **c** The concentration of extracellular ATP was detected by chemiluminescence (n = 3). $^*p < 0.05$ vs. Control group; $^{\#}p < 0.05$ vs. HG group

were reversed by either NPS R568 or spermine (Fig. 7a). In the presence of HG, siRNA-mediated knockdown of CaSR suppressed the stimulatory role of spermine on the total protein levels of Mfn1, Mfn2, and Cx43 (Fig. 7b and c). Immunoprecipitation study further demonstrated that CaSR knockdown attenuated spermine-induced formation of the β-catenin/N-cadherin complex (Fig. 6f). Furthermore, the protective roles of spermine against HG-injured mitochondria length and gap junction intercellular communication were abolished by CaSR-siRNA (Fig. 7e and f). These results clearly indicate that spermine protects mitochondria functions and GJIC by regulating the CaSR-gp78-ubiquitin proteasome system.

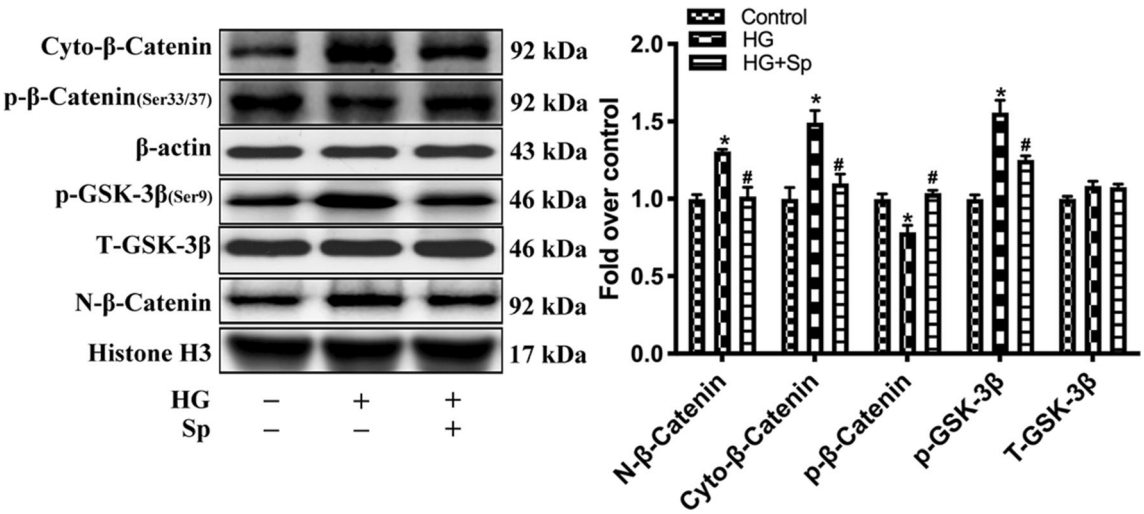

Fig. 5 Exogenous spermine inhibits the phosphorylation of GSK-3β and the nuclear translocation of β-catenin induced by HG. A representative blot was shown. The protein level of N-β-catenin was quantified as a ratio against Histone H3. The protein level of Cyto-β-catenin and p-β-catenin was quantified as a ratio against β-actin. The level of p-GSK-3β was quantified as a ratio against total GSK-3β (n = 3). $^*p < 0.05$ vs. Control group; $^{\#}p < 0.05$ vs. HG group

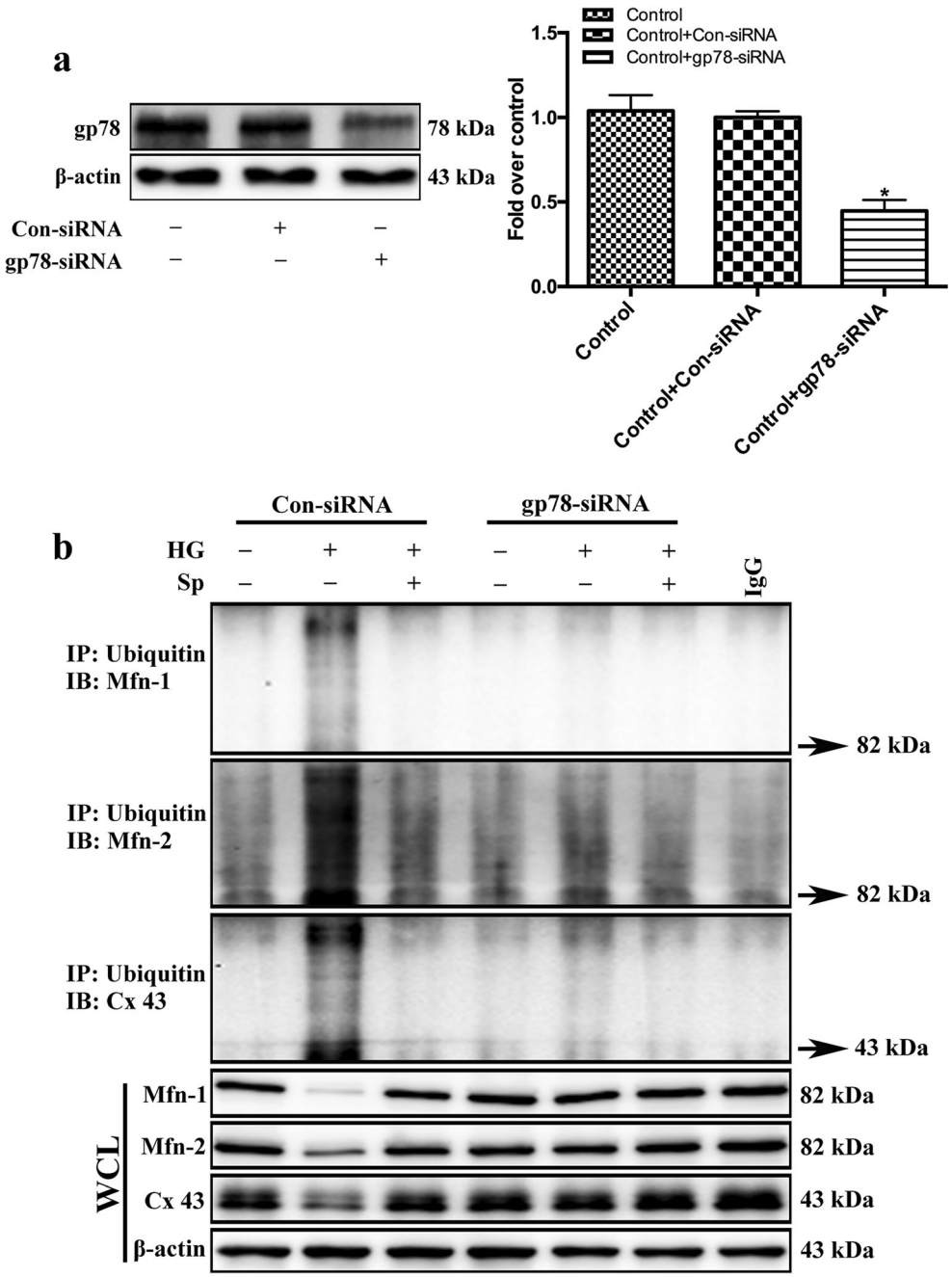

Fig. 6 Exogenous spermine attenuates HG-stimulated gp78-ubiquitin proteasome pathway. **a** Representative western blot of gp78 in cardiomyocytes that were transfected with gp78-siRNA or Con-siRNA (n = 3). **b** The ubiquitination level of Mfn1, Mfn2, and Cx43 in cardiomyocytes that were transfected with gp78-siRNA or Con-siRNA and treated with 5 μM spermine detected using immunoprecipitation (n = 3). *$p < 0.05$ vs. Control group; #$p < 0.05$ vs. HG group

Discussion

The present study explored the intrinsic relationship and the related mechanisms between spermine and energy metabolism in a high glucose-induced cardiomyocyte injury model. We found that (1) HG reduced endogenous spermine content in cardiomyocytes and (2) lower level of spermine then activated myocardial gp78-ubiquitin proteasome system, which hydrolyzes mitochondrial fusion proteins and GJIC-related proteins, resulting in a decreased ATP production and an increased ATP leakage from mitochondria; (3) exogenous spermine could alleviate the myocardial energy metabolism disorder caused by HG. These results uncover an important mechanism for the protective role of spermine against DCM by inhibiting the gp78-ubiquitin protease system.

It has been demonstrated previously that polyamine metabolism is involved in the occurrence and development of cardiovascular diseases, such as myocardial ischemia-reperfusion injury, cardiac hypertrophy and heart failure, but the roles of polyamine, especially spermine, in DCM has not been clarified [19, 28–30]. This study first analyzed the HG-induced alteration of endogenous spermine by looking at the spermine content as well as the protein levels of key enzymes involved in polyamine synthesis and catabolism. We observed

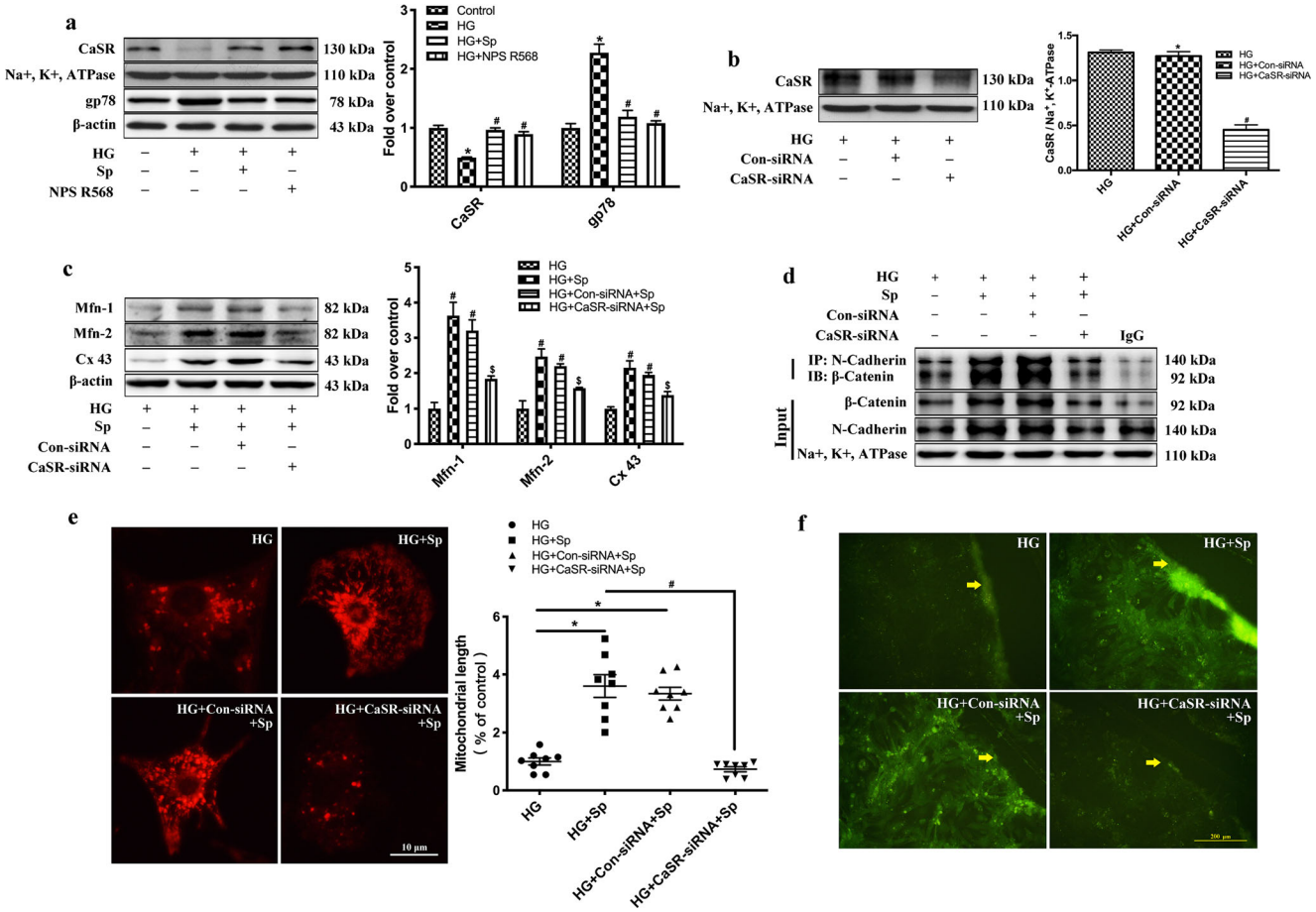

Fig. 7 Exogenous spermine directly or indirectly eliminates HG-induced injury through activating CaSR. **a** Representative western blot of CaSR and gp78 in cardiomyocytes exposed to HG in the presence of 5 μM spermine and 5 μM NPS R568 (n = 3). **b** Representative western blot of CaSR in cardiomyocytes that were transfected with CaSR-siRNA or Con-siRNA (n = 3). **c** Representative western blot of Mfn1, Mfn2, and Cx43 in cardiomyocytes that were transfected with CaSR-siRNA or Con-siRNA (n = 3). **d** The complex level of β-catenin and N-cadherin was detected (n = 3). A typical blot was shown. **e** Morphology of mitochondria was detected by Mito-Tracker and fluorescence microscopy in cardiomyocytes that were transfected with CaSR-siRNA or Con-siRNA and the average length of the mitochondria in each group was quantified. Scale bars = 10 μm ($n = 12$). **f** SLDT was used to detect the function of GJIC. Scale bars = 10 μm (n = 3). The yellow arrow represents the scratch. $^{*}p < 0.05$ vs. Control group; $^{\#}p < 0.05$ vs. HG group; $^{\$}p < 0.05$ vs. HG + Con-siRNA+Sp group

that the content of spermine and the ODC level were significantly reduced, while SSAT level was increased in HG group. Based on these data, it can be inferred that the lower level of ODC and higher level of SSAT in the HG group are the intrinsic factors leading to the disorder of polyamine metabolism. To determine the essential roles of spermine in the development of DCM, we administered exogenous spermine to HG-incubated cardiomyocytes in subsequent experiments. Our previous studies found that exogenous spermine has a double-edged sword effect on cells [31]. In other words, spermine has a protective effect on cells at low concentrations, while at high concentrations, it may cause intracellular calcium overload and lead to cell death. We and others have previously shown that low concentrations of spermine can protect cardiomyocytes by inhibiting endoplasmic reticulum stress, oxidative stress, mPTP opening, and apoptosis [18, 19, 29, 32, 33]. Specifically, it participates in the regulation of intracellular calcium homeostasis [31, 32]. Taken together, spermine plays a wide variety of roles in the physiological and pathological processes of the heart.

In the presence of HG, Mfn1 and Mfn2 protein levels were decreased but Fis1 and Drp1 levels were increased, which led to fragmented mitochondria indicating mitochondrial structural damage. HG also caused the decrease of ΔΨm and mPTP opening. All these changes could be alleviated by spermine co-incubation. We then found that spermine enhanced ATP content in HG-treated cardiomyocytes, consistently, and the protein levels and activities of mitochondrial respiratory chain complexes were also induced by spermine. These data suggest that spermine is essential for maintenance of mitochondrial structure and functions by regulating mitochondrial fusion and fission-related proteins. Gp78, an E3 ubiquitin ligase, often mediates the degradation of various proteins through the ubiquitin-proteasome pathway [34]. We previously

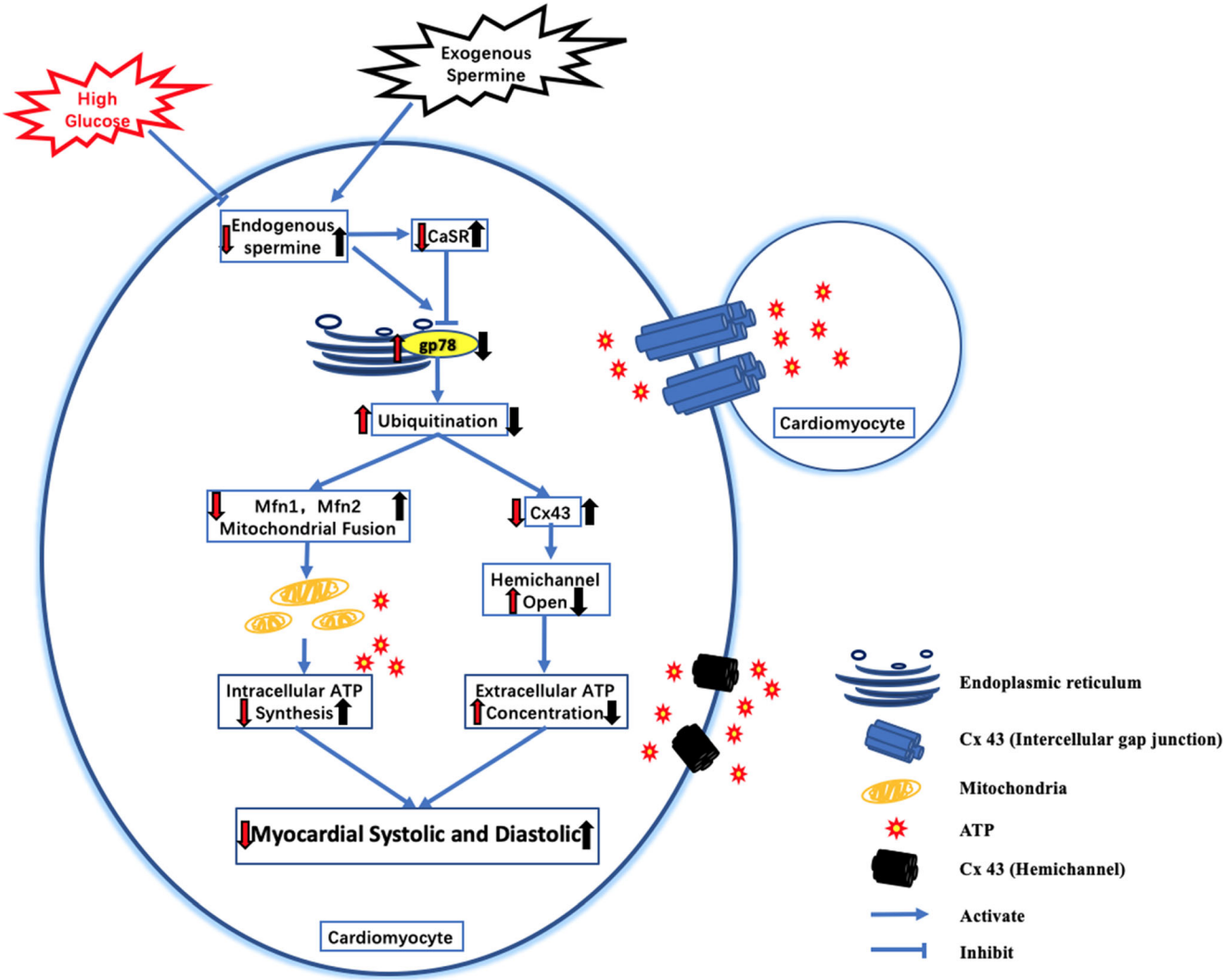

Fig. 8 Schematic diagram on the mechanism of spermine cardioprotection via attenuating HG-induced myocardial energy metabolism disorder by targeting CaSR-gp78-ubiquitination pathways

demonstrated that the increase of gp78 protein level contributed to the energy metabolism disorders in HG-treated cardiomyocytes [8]. We then explored the possible mechanism of involvement of gp78 in HG-induced cardiomyocyte damage. This study provides evidence that spermine can reverse the HG-induced gp78 protein level. Knocking down gp78 expression tlowered the protein levels of Mfn-1, Mfn-2, and Cx43, but their higher degradation via the ubiquitin protease system by HG were significantly suppressed, as also occurred with spermine. This evidence indicate that the blockage of gp78 by spermine alleviates the HG-induced damage of mitochondrial structure and functions.

The present study further confirmed that spermine not only facilitates ATP generation but also inhibits ATP leakage from inside the cells. A decreased production of intracellular ATP or an increased extracellular ATP leakage through the damaged gap junction are often linked to ATP flux disorders. GJIC is a complete cell membrane channel formed by two hemichannels between the adjacent cells, which can transport small metabolites, second messengers, ATP, and electrical signals between cells. GJIC is important for many biological processes, such as growth control, migration, and cell signaling [12, 13, 35]. Cx43, a major component of GJIC, forms a complex with β-catenin and N-cadherin at the myocardial intercalated disk to maintain the normal structure and function of GJIC [36]. Phosphorylation of Cx43, particularly at Ser368 site, can also affect connexin transport and assembly [37]. In this study, the protein levels of Cx43, N-cadherin, and β-catenin in the HG group were significantly reduced, while the phosphorylation levels of Cx43 at Ser368 was significantly increased, indicating the damage of GJIC by HG. The addition of spermine could maintain the protein levels and complexes of GJIC proteins and block the leaking of ATP due to the opening of the hemichannel by HG.

β-catenin is a component of the cell adhesion junction, which is mainly localized on the surface of cytomembrane

but also can translocate to the nucleus and alter transcriptional activity [38, 39]. Abnormally activated Wnt signaling promotes GSK-3β phosphorylation under pathological conditions, which leads to β-catenin dephosphorylation followed by its accumulation in the cytoplasm and then translocation to the nucleus. The present study showed that HG increased GSK-3β phosphorylation and decreased β-catenin phosphorylation, causing the accumulation of β-catenin in the cytoplasm and nucleus of cardiomyocytes. In contrast, the supplement of spermine could reverse these phenomena, possibly by lowering GJIC disruption caused by HG.

CaSR is a member of the G protein-coupled receptor C family and is widely distributed in various tissues and cells [40]. CaSR activation leads to Ca^{2+} release from the sarcoplasmic reticulum through the G protein-PLC-IP3 pathway, and participates in regulating Ca^{2+} homeostasis, cell proliferation, differentiation, and ion channel opening [41, 42]. Accumulated data confirms that CaSR was often involved in myocardial ischemia-reperfusion injury, apoptosis, cardiac hypertrophy, atherosclerosis, pulmonary hypertension, endoplasmic reticulum stress [17, 43, 44]. In the present study, we validated that CaSR protein level was reduced in HG-treated cardiomyocytes but rescued by spermine co-incubation. Similar to the action of spermine, activation of CaSR by its agonist NPS R568 also inhibited the HG-induced gp78 protein level, indicating that CaSR may act as an upstream molecule in mediating the inhibitory role of spermine on gp78 level. This possibility was further supported by the evidence that CaSR knockdown abolished the protective effect of spermine on mitochondria damage and GJIC injury.

In summary, this study confirmed that HG reduced the content of endogenous spermine in cardiomyocytes, which in turn down-regulates CaSR and activates the gp78 ubiquitin-proteasome system followed by ATP flux disruption and cardiomyocyte damage. The supply of exogenous spermine could enhance CaSR protein level, inhibit gp78 activation, and alleviate cardiomyocyte damage induced by HG (Fig. 8). This study demonstrates the protective role of spermine on energy metabolism disorder in HG-treated cardiomyocytes, pointing to the possibility that spermine can be a target for the prevention and treatment of DCM.

Authors' Contributions CW, YHW and YWW designed the research and drafted the manuscript; YHW, YWW, FDL, XXL, and XYZ completed the experiment and data analysis; HZL, GDY, and CQX revised the paper and gave some suggestions. All authors reviewed the results and approved the final version of the manuscript.

Funding This research was supported by the National Natural Science Foundation of China (No. 81800260), University Nursing Program for Young Scholars with Creative Talents in Heilongjiang Province (UNPYSCT), Harbin Medical University Innovation and Entrepreneurship Training Project for College Students (No.201910226010 and No. 201910226448) and Heilongjiang Postdoctoral Fund (No. LBH-Z17103).

Availability of Data and Materials The used and/or analyzed datasets are available from the corresponding author on reasonable request.

Compliance with Ethical Standards

Conflict of Interests The authors declare no potential conflicts of interest with respect to the research, authorship, and/or publication of this article.

References

1. Rubler S, Dlugash J, Yuceoglu YZ, Kumral T, Branwood AW, Grishman A. New type of cardiomyopathy associated with diabetic glomerulosclerosis. Am J Cardiol. 1972;30(6):595–602.
2. Goyal BR, Mehta AA. Diabetic cardiomyopathy: pathophysiological mechanisms and cardiac dysfuntion. Hum Exp Toxicol. 2013;32(6):571–90.
3. Parim B, Sathibabu Uddandrao VV, Saravanan G. Diabetic cardiomyopathy: molecular mechanisms, detrimental effects of conventional treatment, and beneficial effects of natural therapy. Heart Fail Rev. 2019;24(2):279–99.
4. Kohli S, Chhabra A, Jaiswal A, Rustagi Y, Sharma M, Rani V. Curcumin suppresses gelatinase B mediated norepinephrine induced stress in H9c2 cardiomyocytes. PLoS One. 2013;8(10): e76519.
5. Bjornstad P, Schafer M, Truong U, Cree-Green M, Pyle L, Baumgartner A, et al. Metformin improves insulin sensitivity and vascular health in youth with type 1 diabetes mellitus. Circulation. 2018;138(25):2895–907.
6. Dickert N, Sugarman J. Ethical goals of community consultation in research. Am J Public Health. 2005;95(7):1123–7.
7. Raev DC. Which left ventricular function is impaired earlier in the evolution of diabetic cardiomyopathy? An echocardiographic study of young type I diabetic patients. Diabetes Care. 1994;17(7):633–9.
8. Wang Y, Gao P, Wei C, Li H, Zhang L, Zhao Y, et al. Calcium sensing receptor protects high glucose-induced energy metabolism disorder via blocking gp78-ubiquitin proteasome pathway. Cell Death Dis. 2017;8(5):e2799.
9. Marin-Garcia J, Akhmedov AT. Mitochondrial dynamics and cell death in heart failure. Heart Fail Rev. 2016;21(2):123–36.
10. Hom J, Sheu SS. Morphological dynamics of mitochondria–a special emphasis on cardiac muscle cells. J Mol Cell Cardiol. 2009;46(6):811–20.
11. Mahoney VM, Mezzano V, Mirams GR, Maass K, Li Z, Cerrone M, et al. Connexin43 contributes to electrotonic conduction across scar tissue in the intact heart. Sci Rep. 2016;6:26744.
12. Lock JT, Parker I, Smith IF. Communication of ca(2+) signals via tunneling membrane nanotubes is mediated by transmission of inositol trisphosphate through gap junctions. Cell Calcium. 2016;60(4):266–72.
13. Michela P, Velia V, Aldo P, Ada P. Role of connexin 43 in cardiovascular diseases. Eur J Pharmacol. 2015;768:71–6.
14. Harris TJ, Tepass U. Adherens junctions: from molecules to morphogenesis. Nat Rev Mol Cell Biol. 2010;11(7):502–14.
15. Harrison OJ, Bahna F, Katsamba PS, Jin X, Brasch J, Vendome J, et al. Two-step adhesive binding by classical cadherins. Nat Struct Mol Biol. 2010;17(3):348–57.
16. Orellana JA, Froger N, Ezan P, Jiang JX, Bennett MV, Naus CC, et al. ATP and glutamate released via astroglial connexin 43 hemichannels mediate neuronal death through activation of pannexin 1 hemichannels. J Neurochem. 2011;118(5):826–40.
17. Bai SZ, Sun J, Wu H, Zhang N, Li HX, Li GW, et al. Decrease in calcium-sensing receptor in the progress of diabetic cardiomyopathy. Diabetes Res Clin Pract. 2012;95(3):378–85.

18. He Y, Yang J, Li H, Shao H, Wei C, Wang Y, et al. Exogenous spermine ameliorates high glucose-induced cardiomyocytic apoptosis via decreasing reactive oxygen species accumulation through inhibiting p38/JNK and JAK2 pathways. Int J Clin Exp Pathol. 2015;8(12):15537–49.
19. Wei C, Wang Y, Li M, Li H, Lu X, Shao H, et al. Spermine inhibits endoplasmic reticulum stress-induced apoptosis: a new strategy to prevent cardiomyocyte apoptosis. Cell Physiol Biochem. 2016a;38(2):531–44.
20. Fu M, Zhang W, Wu L, Yang G, Li H, Wang R. Hydrogen sulfide (H2S) metabolism in mitochondria and its regulatory role in energy production. Proc Natl Acad Sci U S A. 2012;109(8):2943–8.
21. Connell JP, Augustini E, Moise KJ Jr, Johnson A, Jacot JG. Formation of functional gap junctions in amniotic fluid-derived stem cells induced by transmembrane co-culture with neonatal rat cardiomyocytes. J Cell Mol Med. 2013;17(6):774–81.
22. Sazanov LA. A giant molecular proton pump: structure and mechanism of respiratory complex I. Nat Rev Mol Cell Biol. 2015;16(6):375–88.
23. Meunier B, Fisher N, Ransac S, Mazat JP, Brasseur G. Respiratory complex III dysfunction in humans and the use of yeast as a model organism to study mitochondrial myopathy and associated diseases. Biochim Biophys Acta. 2013;1827(11–12):1346–61.
24. Loiola EC, Ventura AL. Release of ATP from avian Muller glia cells in culture. Neurochem Int. 2011;58(3):414–22.
25. Nazmara Z, Salehnia M, HosseinKhani S. Mitochondrial Distribution and ATP content of vitrified, in vitro matured mouse oocytes, Avicenna. J Med Biotechnol. 2014;6(4):210–7.
26. He Y, Xi J, Zheng H, Zhang Y, Jin Y, Xu Z. Astragaloside IV inhibits oxidative stress-induced mitochondrial permeability transition pore opening by inactivating GSK-3beta via nitric oxide in H9c2 cardiac cells. Oxidative Med Cell Longev. 2012;2012:935738.
27. Gupte SS, Chazotte B, Leesnitzer MA, Hackenbrock CR. Two-dimensional diffusion of F1F0-ATP synthase and ADP/ATP translocator. Testing a hypothesis for ATP synthesis in the mitochondrial inner membrane. Biochim Biophys Acta. 1991;1069(2):131–8.
28. Chai N, Zhang H, Li L, Yu X, Liu Y, Lin Y, et al. Spermidine prevents heart injury in neonatal rats exposed to intrauterine hypoxia by inhibiting oxidative stress and mitochondrial fragmentation. Oxidative Med Cell Longev. 2019;2019:5406468.
29. Wei C, Li H, Wang Y, Peng X, Shao H, Li H, et al. Exogenous spermine inhibits hypoxia/ischemia-induced myocardial apoptosis via regulation of mitochondrial permeability transition pore and associated pathways. Exp Biol Med (Maywood). 2016b;241(14):1505–15.
30. Lin Y, Zhang X, Wang L, Zhao Y, Li H, Xiao W, et al. Polyamine depletion attenuates isoproterenol-induced hypertrophy and endoplasmic reticulum stress in cardiomyocytes. Cell Physiol Biochem. 2014;34(5):1455–65.
31. Han L, Xu C, Jiang C, Li H, Zhang W, Zhao Y, et al. Effects of polyamines on apoptosis induced by simulated ischemia/reperfusion injury in cultured neonatal rat cardiomyocytes. Cell Biol Int. 2007;31(11):1345–52.
32. Hu J, Lu X, Zhang X, Shao X, Wang Y, Chen J, et al. Exogenous Spermine attenuates myocardial fibrosis in diabetic cardiomyopathy by inhibiting endoplasmic reticulum stress and the canonical Wnt signaling pathway. Cell Biol Int. 2020. https://doi.org/10.1002/cbin.11360
33. Wang Y, Chen J, Li S, Zhang X, Guo Z, Hu J, et al. Exogenous spermine attenuates rat diabetic cardiomyopathy via suppressing ROS-p53 mediated downregulation of calcium-sensitive receptor. Redox Biol. 2020;32:101514.
34. Mukherjee R, Chakrabarti O. Ubiquitin-mediated regulation of the E3 ligase GP78 by MGRN1 in trans affects mitochondrial homeostasis. J Cell Sci. 2016;129(4):757–73.
35. Wang N, De Bock M, Decrock E, Bol M, Gadicherla A, Vinken M, et al. Paracrine signaling through plasma membrane hemichannels. Biochim Biophys Acta. 2013;1828(1):35–50.
36. Hertig CM, Butz S, Koch S, Eppenberger-Eberhardt M, Kemler R, Eppenberger HM. N-cadherin in adult rat cardiomyocytes in culture. II. Spatio-temporal appearance of proteins involved in cell-cell contact and communication. Formation of two distinct N-cadherin/catenin complexes. J Cell Sci. 1996;109(Pt 1):11–20.
37. Zou J, Yue XY, Zheng SC, Zhang G, Chang H, Liao YC, et al. Cholesterol modulates function of connexin 43 gap junction channel via PKC pathway in H9c2 cells. Biochim Biophys Acta. 2014;1838(8):2019–25.
38. Bosada FM, Devasthali V, Jones KA, Stankunas K. Wnt/beta-catenin signaling enables developmental transitions during valvulogenesis. Development. 2016;143(6):1041–54.
39. Lee SH, Kim B, Oh MJ, Yoon J, Kim HY, Lee KJ, et al. Persicaria hydropiper (L.) spach and its flavonoid components, isoquercitrin and isorhamnetin, activate the Wnt/beta-catenin pathway and inhibit adipocyte differentiation of 3T3-L1 cells. Phytother Res. 2011;25(11):1629–35.
40. Ray K. Calcium-sensing receptor: trafficking, endocytosis, recycling, and importance of interacting proteins. Prog Mol Biol Transl Sci. 2015;132:127–50.
41. Pidasheva S, Grant M, Canaff L, Ercan O, Kumar U, Hendy GN. Calcium-sensing receptor dimerizes in the endoplasmic reticulum: biochemical and biophysical characterization of CASR mutants retained intracellularly. Hum Mol Genet. 2006;15(14):2200–9.
42. Wang R, Xu C, Zhao W, Zhang J, Cao K, Yang B, et al. Calcium and polyamine regulated calcium-sensing receptors in cardiac tissues. Eur J Biochem. 2003;270(12):2680–8.
43. Sun YH, Liu MN, Li H, Shi S, Zhao YJ, Wang R, et al. Calcium-sensing receptor induces rat neonatal ventricular cardiomyocyte apoptosis. Biochem Biophys Res Commun. 2006;350(4):942–8.
44. Sun J, Wei T, Bai S, Zhao H, Liu X, Yu J, et al. Calcium-sensing receptor-mediated mitogen-activated protein kinase pathway improves the status of transplanted mouse embryonic stem cells in rats with acute myocardial infarction. Mol Cell Biochem. 2017;431(1–2):151–60.

Publisher's Note Springer Nature remains neutral with regard to jurisdictional claims in published maps and institutional affiliations.